Transient-State Real-Time Thermal Rating Forecasting for Overhead Lines by an Enhanced Analytical Method

Fulin Fan*, Keith Bell, and David Infield

Department of Electronic and Electrical Engineering, University of Strathclyde, Glasgow, U.K.

Abstract

The majority of published approaches to real-time thermal rating (RTTR) deal with continuous or steady-state ratings for overhead lines. Less attention has been given to short-term or transient-state RTTRs, partly due to the increased computation time required. This paper describes a fast-computational approach to providing a transient-state RTTR in the form of percentiles based on the predictive distributions modelled for the measured weather variables that are combined with Monte Carlo simulation. An analytical method developed in IEEE Standard 738 calculates the transient-state conductor temperature after a step change in line current only and additionally requires the conductor to be in thermal equilibrium before the step occurs. The IEEE analytical method is enhanced here through inference of an equivalent steady-state initial line current from the initial conductor temperature and weather conditions over a specified time period. Numerous transient-state RTTR forecasts for a particular span are estimated via weather inputs randomly sampled from predictive distributions for a number of time steps ahead combined with the secant method to find the transient-state RTTR. Along with an enhanced analytical method, this yields a maximum allowable conductor temperature for a specified time period under each set of weather samples. The percentiles of transient-state RTTR forecasts are then determined from their sampled values using kernel density estimation. The approach developed here considers variations in weather forecasts at each 10-minute time step.

***Keywords*:** Enhanced analytical method, Overhead lines, Probabilistic forecasting, Real-time thermal rating, Transient state.

* Corresponding author. *E-mail address:* f.fan@strath.ac.uk

1. Introduction

The real-time thermal rating (RTTR) of an overhead line (OHL) is the maximum permissible level of power flow that can pass through the line safely and reliably under prevailing weather conditions. The current-carrying capacity of an OHL is conventionally limited to a static line rating (SLR) [1] which is derived from a maximum allowable conductor temperature T_{cmax} and a conservative set of weather conditions for a particular season based on a thermal model of overhead conductors [2, 3]. RTTR promises to provide additional ampacity; a variety of methods have been proposed to estimate it based on different forms of monitoring and inference with different claims made for their accuracy and cost [4, 5]. However, because actions by a system operator to reduce loading when a thermal limit is reached take time, such re-rating is most useful when augmented by a forecast of the RTTR [6, 7].

Most research related to RTTRs deals only with steady-state ratings which relate to T_{cmax} for specified weather conditions under the assumption that the conductor is in thermal equilibrium. Under transient conditions, the conductor temperature T_c will gradually approach T_{cmax} over a specified short time period (typically less than half an hour) after a step change such as in line current (e.g. due to a system event such an outage of a neighbouring line or a generator) and weather variables considering the conductor's thermal inertia [2, 3]. Although an OHL can be operated at the level of the transient rating for the given short term only, applying transient ratings will provide higher ampacity than using steady-state ratings. Its application is of particular interest in those parts of power systems that are designed to be operated with 'N-1' security as it opens up the possibility of post-event corrective actions rather than having to constrain power flows – and, depending on the nature of the restriction, curtail the output of renewable generators – pre-event, just in case. In effect, transient ratings buy time for the system operator to reduce power flows following an outage down to the steady-state, continuous rating. The cost of actions to re-dispatch generation need only be incurred if and when an unplanned event such as a fault outage occurs rather than, as with pre-event, preventive re-dispatch, at all times [8, 9].

IEEE Standard (Std.) 738 [2] and CIGRE Technical Brochure 601 [3] have both developed

analytical methods to calculate the transient-state T_c as an exponential function of time. This can reduce the computation time compared with the conventional approach [2, 3] which divides the time period (typically 10 minutes) into several sufficiently small time intervals Δt (e.g. 10 seconds) and then estimates the change of T_c over each Δt. However, the IEEE analytical method only considers a step change in line current and requires the conductor to be in thermal equilibrium before the change. In a transient-state calculation example given in [3] where the conventional approach was adopted as a benchmark, the CIGRE analytical method was shown to underestimate T_c by $0.76℃$ at the end of a 10-minute period when an initial steady-state condition was not achieved.

This paper first enhances the IEEE analytical method enabling application to a non-steady-state initial condition and allowing consideration of changes of weather variables. This is done through inference of an equivalent steady-state initial line current from the initial T_c and weather conditions over a specified time period. A weather-based model is then developed to calculate probabilistic forecasts of transient-state RTTRs for a particular future time period (i.e. in this study, 10, 20 and 30 minutes ahead) from correlated weather inputs which are randomly sampled from relevant predictive distributions for up to a half hour (3 steps) ahead generated by conditionally heteroscedastic auto-regressive models that were developed in previous work [6] for air temperature, wind speed and wind direction. Point forecasts of solar radiation are used here instead of probabilistic forecasts since T_c is insensitive to the change in solar radiation when T_c is relatively high [10] or wind speeds are above a modest level [11]. The approach described here additionally uses the secant method to quickly estimate a transient rating that, when using the enhanced analytical method, yields T_{cmax} at the end of the given period under each set of sampled weather conditions.

The ideas are demonstrated here for the 'Drake' conductor and conditions that were used in the CIGRE calculation example in [3] and for two particular 132kV OHL spans in Britain [12] comprising different conductors and in close proximity to installed weather stations. Point forecasts of solar radiation and predictive distributions of other weather parameters for up to three 10-minute time steps over 63 days, from 28/01/2013 to 31/03/2013, have been derived from historic observations at weather stations provided by Scottish Power Energy

Networks from their project of "Implementation of real-time thermal ratings" (LCNF SPT1001) [12]. The paper is structured in the following way: Section 2 describes the methods for T_c modelling and the methodology for transient-state RTTR forecasting; Section 3 assesses the accuracy of T_c estimation by different methods and presents probabilistic forecasts of transient ratings; Section 4 discusses the transient ratings' enhancement over steady-state RTTRs and the need for a safety margin relative to T_{cmax}; and Section 5 presents conclusions and recommendations for further work.

2. Methodology

2.1. Conventional approach & analytical method including enhancement

2.1.1. Conventional approach

For the non-steady-state heat balance equation (HBE) [2, 3] used in the conventional approach to model the transient-state T_c, the variables that depend on T_c, e.g. the ac resistance, convection and radiation heat loss rates per unit length, were evaluated at the initial conductor temperature $T_{ci,\Delta t}$ of each small Δt in the calculation examples given in [2] and [3]. IEEE Std. 738 [2] suggests that it is usually sufficient to select Δt equal to 1% of the conductor's thermal time constant (according to [2], the latter is typically 5 – 20 minutes) and that a Δt equal to 10-second or less is a reasonable choice to ensure accuracy in iterative calculations. However, this comes at the cost of high computation time.

An alternative approach is to evaluate the T_c dependent variables at the average $T_{cav,\Delta t}$ of the initial and final conductor temperatures over each Δt. Because of the dependency of some variables on T_c, the latter is iteratively adjusted over each Δt until both sides of the non-steady-state HBE are equal. This approach is expected to give more accurate T_c estimates than the $T_{ci,\Delta t}$-based approach, again at the cost of extra computation time.

2.1.2. IEEE and CIGRE analytical method

Assuming an initial steady-state condition and the cooling terms in the non-steady-state HBE to be linear with T_c, the IEEE analytical method developed in [2] calculates the transient-state T_c after the change of line current only as an exponential function of time:

$$T_c(t) = T_{ci} + \left(T_{ss,cf} - T_{ci}\right) \cdot \left(1 - e^{-t/\tau}\right) \quad (1)$$

where the thermal time constant τ is approximated as:

$$\tau = \left[\left(T_{ss,cf} - T_{ci}\right) \cdot H(T_{cav})\right] / \left[R(T_{cav}) \cdot \left(I_f^2 - I_i^2\right)\right] \quad (2)$$

where the conductor's ac resistance R and heat capacity H per unit length are evaluated at the average $T_{cav} = \left(T_{ci} + T_{ss,cf}\right)/2$ of the initial conductor temperature at the start of a given time period T_{ci} and the steady-state final conductor temperature $T_{ss,cf}$ that is estimated from weather conditions and the line current I_f after a step change. Magnetic heating effects may also be significant for single- or three-aluminium-layer steel-cored conductors [2, 3] and should normally be taken into account. However, they can be neglected for the conductors studied in this paper which are all aluminium alloy conductor (AAAC) or aluminium conductor steel-reinforced (ACSR) with two aluminium layers where, according to [2] and [3], the magnetic effect essentially cancels out and the level of magnetic flux in the steel core is quite low.

The CIGRE analytical method [3] estimates the non-negative thermal time constant τ_x for the step change in each of the heating and cooling terms ΔQ_x separately:

$$\tau_x = \left|\left(T_{ss,cf} - T_{ci}\right) \cdot H(T_{ci}) / \Delta Q_x\right| \quad (3)$$

and then determines T_c as an exponential function of time [3]:

$$T_c(t) = T_{ci} + \left(T_{ss,cf} - T_{ci}\right) \cdot \left(1 - e^{-\left(t/\tau_J + t/\tau_s + t/\tau_c + t/\tau_r\right)}\right) \quad (4)$$

where terms τ_J, τ_s, τ_c and τ_r represent thermal time constants for the changes in rates of Joule heat gain, solar heat gain Q_s, convection heat loss Q_c and radiation heat loss Q_r per unit length respectively. For further details of the methods used in the present study to calculate heat gain, loss terms and air properties (e.g. dynamic viscosity and thermal conductivity of air), the reader is referred to IEEE Std. 738 [2].

2.1.3. Enhanced analytical method

To create the conductor's thermal equilibrium at the start of a specified time period as required by the IEEE analytical method, the enhanced method infers an equivalent steady-state initial line current $I_{i,eq}$ from T_{ci} and weather conditions wc over the time period based on the steady-state HBE [2]:

$$I_{i,eq}^2 = \left[Q_c(T_{ci}, wc) + Q_r(T_{ci}, wc) - Q_s(wc)\right] / R(T_{ci}) \quad (5)$$

Then the term I_i^2 in equation (2) is replaced with the inferred $I_{i,eq}^2$ to determine τ and T_c. In this manner, the transient-state impact of the actual line current and weather conditions

prior to the step change on the conductor is converted into the steady-state influence of $I_{i,eq}$ and wc. As a result, the enhanced analytical method successfully takes changes of weather conditions into account.

2.2. The secant method

Since $T_{ss,cf}$ cannot be directly solved from wc and I_f via the steady-state HBE [2], the value of $T_{ss,cf}$ has to be iteratively adjusted until the calculated line current equals the given I_f. The use of a root-finding algorithm can quickly estimate $T_{ss,cf}$ and effectively reduces computation time. Since it is difficult to evaluate the derivative of the steady-state HBE with respect to T_c, the secant method approximating the derivative by secant lines [13] appears preferable to Newton's method and has been used in this study. When using the secant method to determine $T_{ss,cf}$, the function F_1 of $T_{ss,cf}$ is defined as the difference between the square of the given I_f and the square of the steady-state current calculated from an assumed $T_{ss,cf}$ and wc. A termination criterion of $\left|F_1\left(T_{ss,cf}\right)\right| < 0.1A^2$ is found in the tests conducted here to be sufficient for the secant method to give an accuracy of 1×10^{-4}℃. Two initial iterations are carried out at the air temperature and T_{cmax}.

The secant method is also used to adjust the transient rating I_{ts} until the calculated transient-state final conductor temperature $T_{ts,cf}$ reaches T_{cmax} at the end of a given time period. The function F_2 of I_{ts} is defined as the deviation between T_{cmax} and $T_{ts,cf}$ that is estimated from the assumed I_{ts}, T_{ci} and wc using the enhanced analytical method. The iterative calculation is terminated when $|F_2(I_{ts})| < 0.001$℃.

2.3. Correlating weather input variables for RTTR estimation

2.3.1. Rank correlation based pairing

In order that a system operator can make an informed judgment on the risk associated with a forecast of a rating, they should be provided with a probabilistic forecast that quantifies not only the central forecast value but also the error likelihood. Since it is difficult to directly estimate probabilistic RTTR forecasts from predictive distributions of weather parameters, in this case, Monte Carlo simulation [14] is used to generate a large number (10^4) of sampled values of transient rating forecasts that are determined from weather input variables randomly sampled from the predictive distributions modelled for air temperature, wind speed and wind

direction combined with point forecasts of solar radiation.

Numerous weather samples generated from the independent predictive distributions for up to three 10-minutes time steps ahead are found to be not correlated with each other. A rank correlation based pairing method detailed in [15] is used here to pair random samples of air temperature and wind speed at the same and different future moments so as to create a correlation similar to that computed from their recent observations.

2.3.2. Transient-state RTTR estimation and constraints

Changes in weather forecasts at each future time (up to 3 steps ahead) are considered. Given an assumed 30-minute RTTR forecast $I_{ts,3}$, the 1-step-ahead weather forecasts wf_1 are first used to estimate the growth in T_c from the initial temperature T_{ci} to T_{c10} at the end of the first future 10 minutes, which then increases to T_{c20} at the end of the second future 10 minutes under the 2-step-ahead weather forecasts wf_2; the 3-step-ahead weather forecasts wf_3 are finally used to calculate the increase in T_c from T_{c20} to T_{c30}.

A higher level of transient rating is generally obtained for a shorter time period. The relationships among transient ratings for up to a half hour ahead, $I_{ts,1}$, $I_{ts,2}$ and $I_{ts,3}$, should be such that $I_{ts,1} \geq I_{ts,2} \geq I_{ts,3}$. Otherwise, T_{cmax} would be exceeded. In some extreme cases where, for example, wf_3 provide more significant cooling on the conductor than wf_2, the calculated $I_{ts,3}$ may be greater than $I_{ts,2}$, which leads to T_c exceeding T_{cmax} at the end of the 20 minute period and then reducing to T_{cmax} at the end of 30 minutes. Therefore, values of $I_{ts,2}$ and $I_{ts,3}$ must be limited to the calculated $I_{ts,1}$ and the calculated or restricted $I_{ts,2}$ respectively so as to avoid the risk of T_{cmax} being exceeded in such extreme cases.

In each of 10^4 scenarios generated by Monte Carlo simulation, two initial iterations in the secant method for estimating the sampled value of $I_{ts,1}$ are carried out at the calculated 10-minute-ahead steady-state rating $I_{ss,1}$ and $1.5I_{ss,1}$. When estimating the sampled values of $I_{ts,2}$ and $I_{ts,3}$, two initial iterations are carried out at the calculated 20-minute-ahead steady-state rating $I_{ss,2}$ and $I_{ts,1}$, and the 30-minute-ahead steady-state rating $I_{ss,3}$ and $I_{ts,2}$ respectively. The percentiles of $I_{ts,1}$, $I_{ts,2}$ and $I_{ts,3}$ are then estimated from their respective 10^4 sampled values separately by kernel density estimation [16].

In summary, the inputs of the weather-based model developed in this paper for the transient rating forecasting are T_{ci}, T_{cmax}, historic weather observations (i.e. wind speed, wind direction, air temperature and solar radiation) and the set of parameters representing the conductor's characteristics. Along with the model's outputs of probabilistic forecasts or predictive percentiles of transient ratings for different horizons, predictive distributions of weather conditions and steady-state ratings are produced as intermediate data.

3. Results and model validation

All mathematical calculations in the work presented here are undertaken using MATLAB [17]. The accuracies of conventional approaches and analytical methods in the transient-state T_c modelling will be assessed first, followed by detailing of the process of estimating probabilistic forecasts of 10-minute, 20-minute and 30-minute transient ratings.

3.1. Assessment of conventional and analytical methods

The influence of Δt on the two conventional approaches, i.e. evaluating T_c dependent variables at $T_{ci,\Delta t}$ or $T_{cav,\Delta t}$ over each Δt, is assessed here based on the experimental data used in the calculation example given in [3], as listed in Table 1. The technical parameters describing characteristics of the 'Drake' conductor used in the calculation example in [3] are listed in the Appendix below.

Table 1. *Weather data and line currents in three subsequent 10-minute periods [3].*

Time Periods (hh:mm)	Air Temp. (℃)	Wind Speed (m/s)	Attack Angle (deg)	Solar radiation (W/m^2)	Line current (A)
Prior to 00:00	24.0	1.9	55	0	802
00:00 – 00:10	23.7	1.7	62	0	819
00:10 – 00:20	23.5	0.8	37	0	856

The transient-state T_c modelled by different conventional approaches that use $T_{ci,\Delta t}$ or $T_{cav,\Delta t}$ with a 10-second or 1-minute Δt are compared in Fig. 1(a). The analysis results show that 1) given a relatively significant growth in line current and/or reduction in wind cooling on the conductor, the conventional approach that uses $T_{ci,\Delta t}$ with a 1-minute Δt will overestimate T_c due to the cooling terms evaluated at $T_{ci,\Delta t}$ being underestimated over Δt; and 2) the use of $T_{cav,\Delta t}$ leads to the conventional approaches with different Δt being both reasonably accurate and conservative in this case.

Fig. 1(b) shows the transient-state T_c modelled using the CIGRE analytical method and the enhanced analytical method. A conventional approach that uses $T_{cav,\Delta t}$ with a 10-second Δt is adopted as a benchmark. Both analytical methods estimate the heating and cooling terms in equations (3) and (5) using the IEEE formulae described in [2].

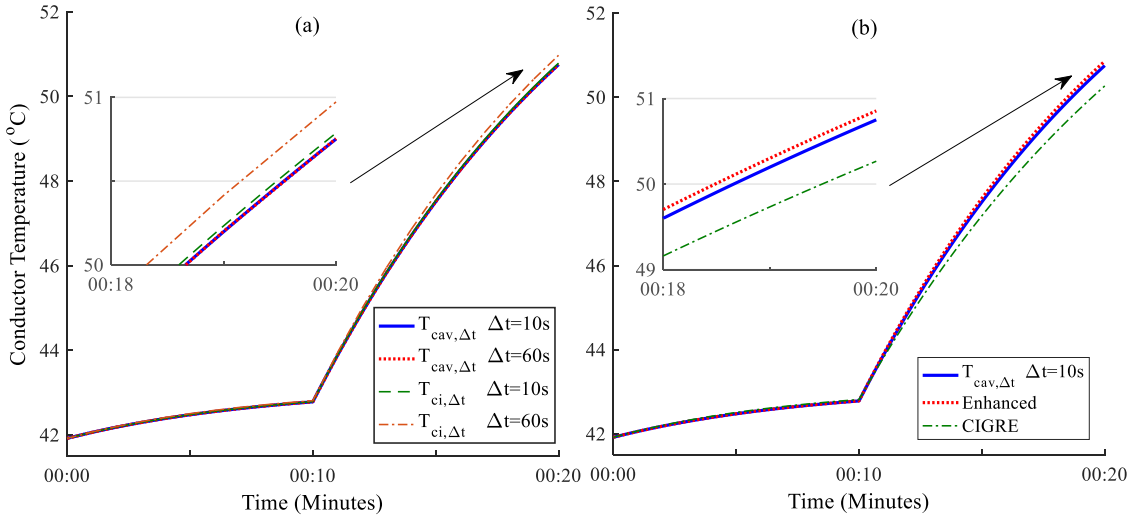

Fig. 1. *Transient-state temperatures of the 'Drake' conductor modelled by (a) different conventional approaches, and (b) the enhanced analytical method and the CIGRE analytical method.*

The conductor temperature at 00:20, $T_c(00{:}20)$, modelled by the CIGRE method is found to be 0.7℃ lower than that estimated by the conventional approach using $T_{ci,\Delta t}$ with a 1-minute Δt. The deviation is very close to the error obtained in the calculation example given in [3]. Compared with the benchmark adopted here, the CIGRE method underestimates $T_c(00{:}20)$ by about 0.48℃ while the enhanced method overestimates $T_c(00{:}20)$ by around 0.1℃. The less accurate estimate of $T_c(00{:}20)$ by the CIGRE method may be due to it requiring the conductor to be in thermal equilibrium before a step change in conditions occurs. To test this, a steady-state condition at 00:10 is created by assuming that the line current and weather conditions remain at their initial values up to 00:10 and then change to the values specified for 00:10-00:20. In this case, the difference between $T_c(00{:}20)$ for the two analytical methods is only about 0.056℃.

It is found that, under the assumption of the cooling terms linearly varying with $T_c \in [T_{ci}, T_{ss,cf}]$, the enhanced analytical method evaluating the ac resistance R at $T_{cav} = (T_{ci} + T_{ss,cf})/2$ would overestimate/underestimate instantaneous values of the heat gain rate and the linearized heat loss rate per unit length at T_c by $\Delta Gain(T_c)$ and

$\Delta Loss_{linearized}(T_c)$ respectively, which have a non-negative difference:

$$\Delta Gain(T_c) - \Delta Loss_{linearized}(T_c) = \left(I_f^2 - I_{i,eq}^2\right) \cdot \frac{R\left(T_{ss,cf}\right) - R(T_{ci})}{2} \cdot \left(\frac{T_{ss,cf} - T_c}{T_{ss,cf} - T_{ci}}\right) \geq 0 \qquad \forall\, T_c \in \left[T_{ci}, T_{ss,cf}\right] \tag{6}$$

Equation (6) is also applied to the case where $T_c \in \left[T_{ss,cf}, T_{ci}\right]$ decreases from T_{ci} after a reduction in line current from $I_{i,eq}$ to I_f. The non-negative difference between $\Delta Gain(T_c)$ and $\Delta Loss_{linearized}(T_c)$ means that the transient-state conductor temperature at the end of a specified time period would be overestimated by the enhanced analytical method given a relatively slight overestimation in the cooling terms after the linearization.

3.2. Transient-state conductor temperature modelling

The transient-state T_c of spans CQ34-CQ35 and AC102-AC101B in close proximity to installed weather stations are studied. They comprise 'Lynx' ACSR $175mm^2$ and 'Poplar' AAAC $200mm^2$ conductors with T_{cmax} of 50℃ and 75℃ respectively, which are reduced by 5℃ to provide a safety margin [12]. The technical parameters describing the characteristics of 'Lynx' and 'Poplar' conductors are listed in the Appendix below. The transient-state T_c estimated from the measured line current and weather data by the conventional approach using $T_{cav,\Delta t}$ with a 10-second Δt is regarded as the 'actual' T_c and used as a benchmark. To compare the accuracy and computation time of the enhanced analytical method and the $T_{ci,\Delta t}$-based conventional approach with a 10-second Δt, the changes of T_c over each 10-minute period for different spans are calculated by the two methods based on the 'actual' initial conductor temperatures at the start of the period that are combined with the corresponding measured weather data and line currents. The distributions of errors of the transient-state final conductor temperature $T_{ts,cf}$ at the end of the 10-minute period modelled by the two methods during 28/01/2013 to 31/03/2013 for different spans are shown in Fig. 2. The average computation time used by the $T_{ci,\Delta t}$-based conventional approach with a 10-second Δt and the enhanced method is about $4.5 \times 10^{-3}s$ and $5.4 \times 10^{-4}s$ respectively. (The computer being used has a 64-bit operating system, 4GB of RAM, Intel Core i5-3470 3.2GHz processor).

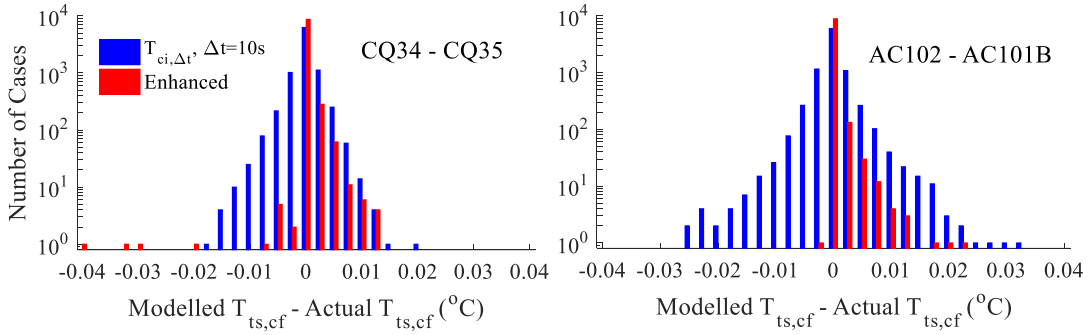

Fig. 2. *Distribution of $T_{ts,cf}$ errors modelled by the $T_{ci,\Delta t}$-based conventional approach and the enhanced analytical method for different spans.*

The $T_{ci,\Delta t}$-based conventional approach is found to overestimate the growth or reduction in $T_{ts,cf}$ to different extents, depending on the level of changes in line current and weather conditions. The enhanced method is shown to produce slightly more accurate estimates of $T_{ts,cf}$ over the evaluated period. Furthermore, as noted in Section 3.1, $T_{ts,cf}$ modelled by the enhanced method is greater than or equal to the 'actual' value for most of the time due to the non-negative difference between $\Delta Gain(T_c)$ and $\Delta Loss_{linearized}(T_c)$ and a relatively slight overestimation in the cooling terms after the linearization. However, the enhanced method underestimates $T_{ts,cf}$ by greater than 0.02℃ in some particular cases where Q_c evaluated at T_{ci} and $T_{ss,cf}$ were found to be determined by the forced Q_{cf} and the natural convection heat loss rates Q_{cn} respectively. (IEEE Std. 738 [2] recommends that Q_c is determined as the larger of Q_{cn} and Q_{cf}). Fig. 3(a) shows the growths of Q_{cn}, Q_{cf} and the linearized Q_c (denoted by $Q_{c,linearized}$) with $T_c \in [T_{ci}, T_{ss,cf}]$ in a particular case where $T_{ts,cf}$ of span CQ34-CQ35 over 18:20-18:30 on 16/03/2013 was underestimated by the enhanced method; the values of $(\Delta Gain(T_c) - \Delta Loss_{linearized}(T_c))$ and overestimations in $Q_c(T_c)$ and $Q_r(T_c)$ after the linearization are then compared in Fig. 3(b). Before T_c reached $T_{ts,cf}$, $(\Delta Gain(T_c) - \Delta Loss_{linearized}(T_c))$ was much greater than the overestimation in $Q_r(T_c)$, but significantly exceeded by the overestimation in $Q_c(T_c)$ when T_c was above a certain level in this case. The total overestimation in Q_c and Q_r after the linearization exceeding $(\Delta Gain - \Delta Loss_{linearized})$ over a given time period would lead to an underestimated $T_{ts,cf}$ at the end of the time period.

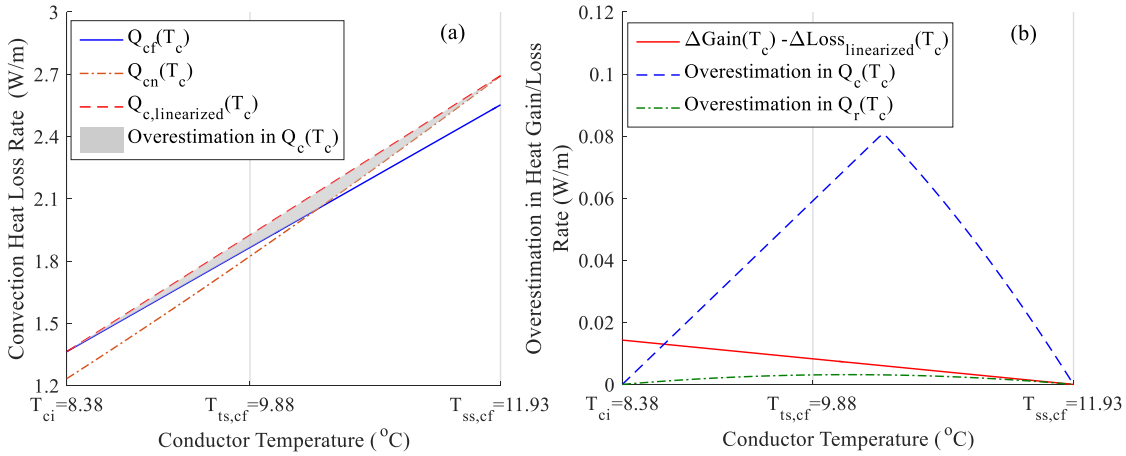

Fig. 3. (a) Variations in the forced, natural and linearized convection heat loss rates with T_c and (b) a comparison of $(\Delta Gain - \Delta Loss_{linearized})$ against the overestimations in convection and radiation heat loss rates after the linearization for span CQ34-CQ35 over 18:20-18:30 on 16/03/2013.

3.3. *Enhanced analytical method based RTTR estimation*

The transient rating determined for a given short period based on the enhanced analytical method is usually conservative since, as noted above, the enhanced method is likely to overestimate the growth in $T_{ts,cf}$ after an increase in line current. Fig. 4 shows the distributions of differences between T_{cmax} and the 'actual' $T_{ts,cf}$ at the end of the given time periods under the 10-minute, 20-minute and 30-minute RTTRs that are estimated from weather observations using the enhanced method for the two spans. (The cases of 20-minute and 30-minute RTTRs being restricted are omitted here simply for brevity).

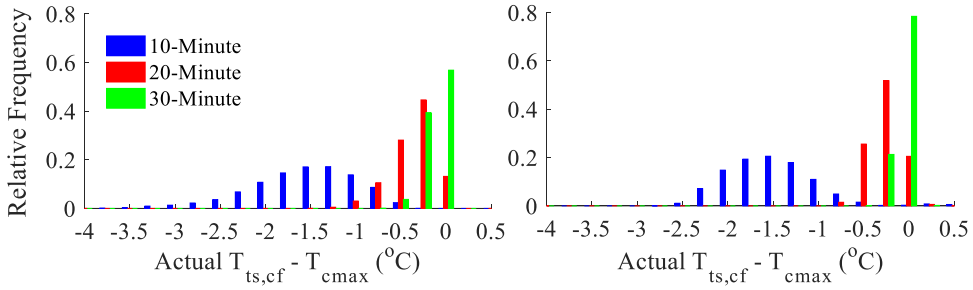

Fig. 4. *Distributions of differences between T_{cmax} and the 'actual' $T_{ts,cf}$ at the end of 10-, 20- and 30-minute periods under the enhanced analytical method based transient ratings for two spans.*

The final temperature of the conductor operated at the level of the enhanced method based transient rating, especially the 10-minute rating, does not reach T_{cmax} for the majority of the time. A smaller deviation from T_{cmax} is mostly observed at the end of the 30-minute period since the conductor has a long time to respond to the significant increase in line current.

It is noted that T_{cmax} is slightly exceeded in a few cases due to the overestimated Q_c and Q_r as discussed in Section 3.2. Fortunately, the created 5℃ safety buffer relative to the original maximum limit is greater than these exceedances.

3.4. Assessment of probabilistic RTTR forecasting

In Monte Carlo simulation, random samples of air temperature and wind speed, generated from the predictive distributions for up to a half hour (3 steps) ahead modelled in [6] over a particular future half-hour period, are paired to create rank correlations close in value to those between their observations within the most recent 15 days, as shown in Fig. 5 for the span CQ34-CQ35. (See the Appendix for relevant conductor parameters).

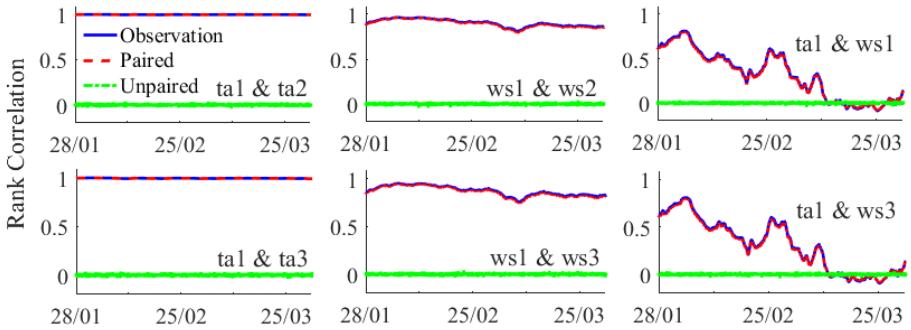

Fig. 5. *Rank correlations between unpaired, paired random samples of air temperature and wind speed forecasts for up to 3 steps ahead (i.e.* ta_i *and* ws_i, $i = 1, 2, 3$*) and their recent observations within 15 days at span CQ34 – CQ35.*

The sampled values of $I_{ts,1}$, $I_{ts,2}$ and $I_{ts,3}$ are determined from the independent and correlated random samples of air temperature and wind speed separately that are combined with independent wind direction samples and point forecasts of solar radiation for up to a half hour ahead during a particular future 30-minute period in each of the 10^4 scenarios. The cumulative distribution function (CDF) extracted from sampled values of the rating forecast is then smoothed by kernel density estimation [16] to estimate predictive percentiles for each time horizon. Figs. 6 and 7 show the ratios of transient-state RTTRs to the SLRs on 27/03/2013 for the two spans respectively. The transient ratings are based, in turn, on the correlated weather samples based 5th – 95th percentiles, 25th – 75th percentiles, point forecasts of 10-minute and 30-minute RTTRs and weather observations.

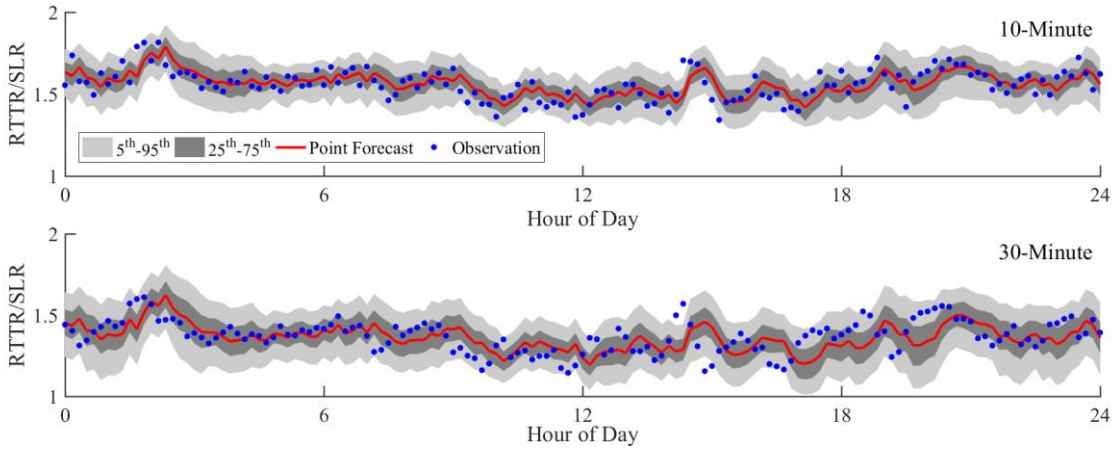

Fig. 6. *Probabilistic forecasts of 10-minute and 30-minute RTTRs on 27/03/2013 for CQ34-CQ35.*

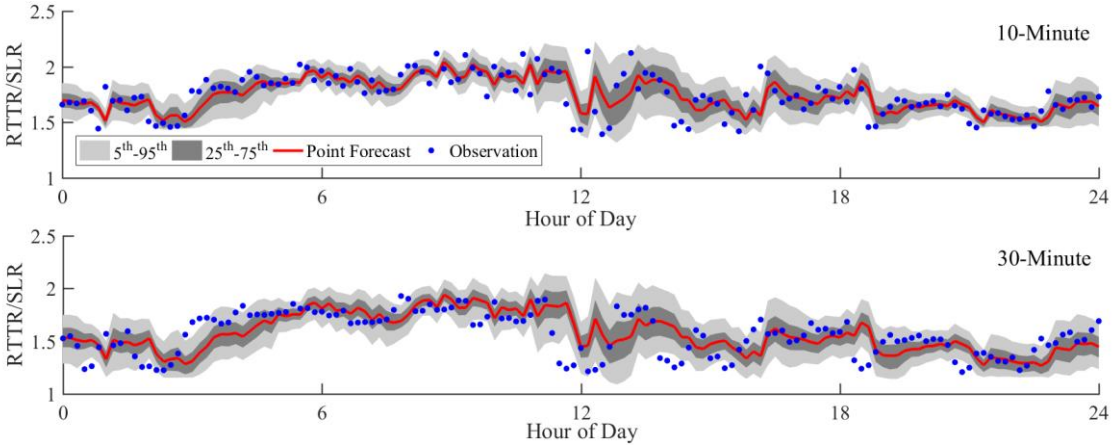

Fig. 7. *Probabilistic forecasts of 10-minute and 30-minute RTTRs on 27/03/2013 for AC102-AC101B.*

The predictive distributions of 30-minute ratings are shown to be less concentrated than that of 10-minute ratings on average. This is because the forecast accuracy decreases with increasing look ahead and the uncertainties of weather forecasts for up to a half hour ahead are all included for estimation of the possible errors of a 30-minute rating forecast.

The transient ratings estimated from persistence forecasts of weather conditions, which are assumed to be constant within the upcoming period, are adopted as benchmarks to assess the accuracy of the point RTTR forecasts generated by the conditionally heteroscedastic (CH) models [6] based on correlated (CH-C) weather samples. The point forecasts of the CH-C model based $I_{ts,1}$ and $I_{ts,3}$ having root mean square errors (RMSEs) of $36A$ and $47A$ respectively give 11% and 18.2% improvements over the persistence forecast based ratings for CQ34-CQ35. The corresponding RMSEs for AC102-AC101B are $47.7A$ and $62A$ respectively which give 9% and 17.6% improvements over persistence. Though performing better than the persistence forecasting on average, the CH-C model is usually found to

overestimate transient ratings for both spans at the levels of their respective lower ratings (e.g. the smallest 5% of weather observation based ratings). The lower percentiles should therefore be applied so as to avoid the risk of using the overestimated point forecasts of the CH model based transient ratings.

To assess the calibration of probabilistic transient rating forecasts, histograms of the probability integral transform (PIT) that is the value of the predictive CDF evaluated at the observation [6] are plotted for RTTR forecasts of two spans which are derived from the independent (CH-I) and correlated (CH-C) weather samples separately, as shown in Figs. 8 and 9. The relative frequency of 0.01 per percentile for a uniform PIT histogram which reveals probabilistic forecasts to be fully calibrated is denoted by a black solid line.

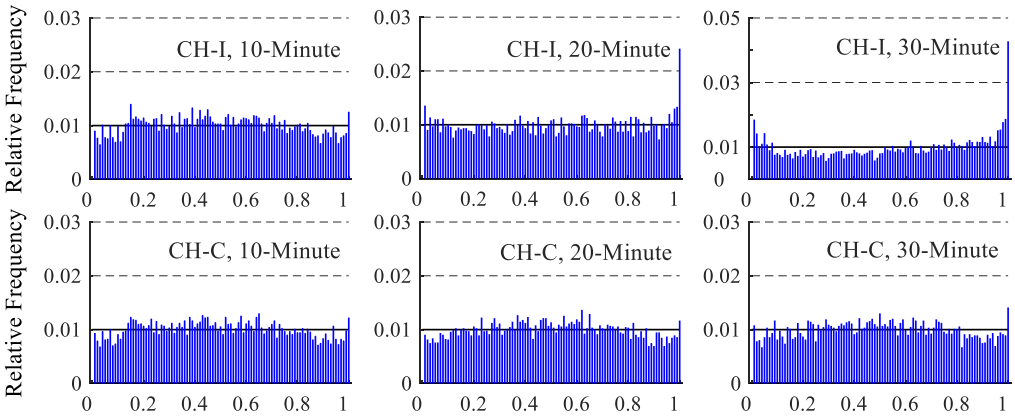

Fig. 8. *PIT histograms of probabilistic transient-state RTTR forecasts for CQ34-CQ35.*

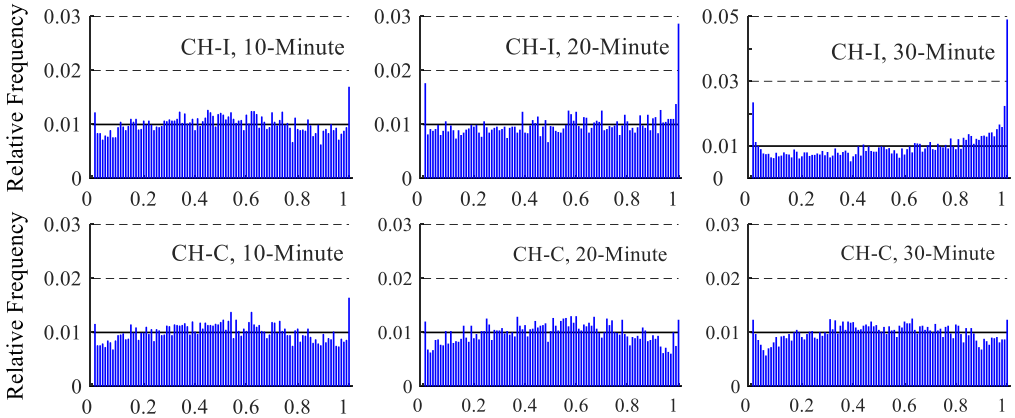

Fig. 9. *PIT histograms of probabilistic transient-state RTTR forecasts for AC102-AC101B.*

The relative frequencies at both ends of CH-C PIT histograms of $I_{ts,1}$ forecasts are similar to those for CH-I PIT histograms. Though the paired samples of one-step-ahead air temperature and wind speed forecasts showing long-term positive correlations have opposite

cooling effects, their correlations may have a slight impact on the dispersion of predictive distributions of $I_{ts,1}$ due to the relatively high accuracy of air temperature predictions [18]. For $I_{ts,2}$ and $I_{ts,3}$ forecasts, the significant deviations from the ideal relative frequency of 0.01 at both ends of CH-I PIT histograms are successfully mitigated in CH-C PIT histograms. This is because the paired random samples of the same weather parameter at different future moments (up to 30 minutes ahead) that, in each of the 10^4 scenarios, show significant positive correlations will be at similar levels with respect to their respective ranges of the 10^4 random samples; the low wind speed forecasts or the high air temperature forecasts assigned to different future moments in a particular scenario would lead to the calculated $I_{ts,2}$ and $I_{ts,3}$ forecasts being at a certain low level, and vice versa. This means that the predictive distributions of $I_{ts,2}$ and $I_{ts,3}$ estimated from the paired weather samples are commonly more dispersive than those based on the unpaired random samples. Therefore, predictive percentiles of transient ratings modelled based on the paired weather samples randomly generated from the CH forecasting models are preferred here due to their improved calibration, especially at lower percentiles.

4. Discussion

The duration that a conductor can be operated at the level of the calculated steady-state RTTR is generally determined by the frequency at which the rating is updated. For example, the conductor's ampacity would be assumed to be kept at the hourly updated steady-state RTTR over the present or future one hour. However, the use of weather data averaged over a relatively longer interval, e.g. one hour, may lead to a risk of the conductor's thermal overloading due to the short-term variability of weather conditions, especially wind speed [19]. It is recommended that an update interval of 10 minutes is preferred to fulfil the requirement of rating calculation for most cases [19, 20].

Given time for SCADA measurements to be received, a system state estimation to be updated and some consideration of the implications of the system's state relative to prevailing and anticipated ratings, a forecast horizon of 30 minutes is sufficient for a system operator to take action based on the forecast result. Considering the fast computation of steady-state ratings, a system operator is likely to be provided with a steady-state RTTR forecast that can

last for 30 minutes. To avoid the risk of overheating a conductor in between rating updates, the minimum value of steady-state RTTR forecasts for up to three 10-minutes time steps ahead could be adopted as the thermal limit for the future half hour. Furthermore, as is argued in [6] and was noted in Section 2.3 above, a forecast should not be of just a single value at each future point in time but of a distribution. This would allow the system operator to choose a value from the distribution that allows them to feel suitably confident about the associated risks.

The transient rating is mostly found in the tests conducted here to offer higher additional headroom of conductor ampacity than the minimum value of steady-state RTTRs for different time horizons, as shown in Fig. 10 where the rating calculations are based on weather observations. The enhancement over steady-state RTTRs decreases with increases with forecast look ahead time, e.g. the median increases provided by the weather observation based $I_{ts,1}$ and $I_{ts,3}$ are 11.4% and 4.8% for CQ34-CQ35, and 8% and 3.1% for AC102-AC101B respectively in this work. Furthermore, the probabilistic approach developed here that uses an enhanced analytical method combined with the secant method requires around 2 seconds to compute forecasts of $I_{ts,1}$, $I_{ts,2}$ and $I_{ts,3}$ for 2×10^4 scenarios, which is smaller than about the roughly 20 seconds needed by the one using the $T_{ci,\Delta t}$-based conventional approach with a 10-second Δt. (The 2×10^4 calculations are simultaneously processed through the matrix calculation realised in MATLAB). The short time required for the transient-state calculation increases the practicability of applying the lower percentiles of transient-state RTTR forecasts.

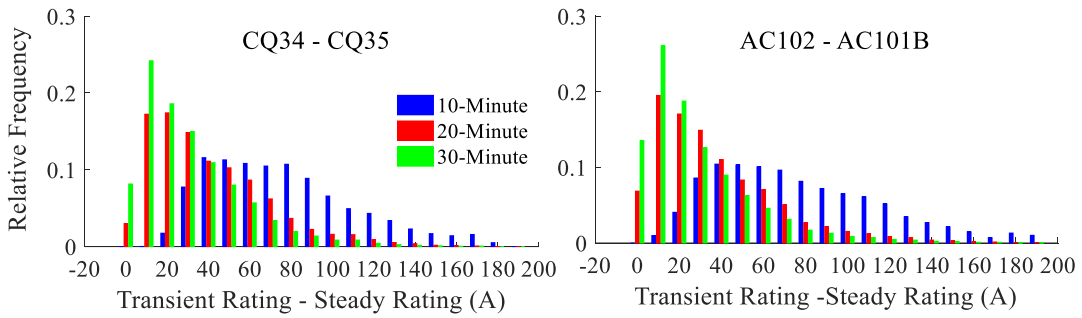

***Fig. 10**. Distributions of differences between transient-state ratings and the minimum values of steady-state ratings for different time horizons for different spans which are calculated based on weather observations*

Even though the installed station is very close to the span, the weather-based model that directly estimates RTTRs from weather data may suffer from the difference between the wind conditions recorded at a weather station and those actually experienced by the conductor leading to an inaccurate calculation of the convection heat loss rate. To address this, an 'effective' wind speed perpendicular to the span is usually estimated from the monitored or inferred conductor temperature combined with measurements of the line current, air temperature and solar radiation, and then used with T_{cmax} to calculate RTTRs based on a thermal model of overhead conductors [4]. Furthermore, considering the accuracy of monitoring instrumentation, a correction factor can be applied to weather measurements based on the equipment specification sheets to ensure a conservative rating estimation [12]. However, the parameters describing the conductor's emissivity ϵ and absorptivity α that respectively determine rates of radiation heat loss and solar heat gain are usually coarsely estimated. Although the transient rating estimated by the enhanced method is mostly conservative in this study, an overestimated ϵ or an underestimated α may lead to the transient-state final conductor temperature $T_{ts,cf}$ exceeding T_{cmax} at the end of the given time period. Fig. 11 shows cumulative frequency distributions of deviations between T_{cmax} and $T_{ts,cf}$ that are modelled by the $T_{cav,\Delta t}$-based conventional approach with a 10-second Δt under the weather observation based transient ratings for different time horizons for the two spans, assuming the actual value of ϵ or α to be 0.1 or 0.2 smaller or greater than that used in this work. Since ϵ of energized conductors is highly correlated with α and generally considered to be slightly higher than α [20], the combinations of ϵ and α tested here (i.e. ϵ/α equalling 0.5/0.7 or 0.4/0.6 for CQ34-Q35 and 0.8/0.9 or 0.7/0.9 for AC102-AC101B) are expected to give the worst cases of T_{cmax} being exceeded. Therefore, a reasonable safety margin relative to the original maximum temperature limit is necessary for the transient rating calculation in this study.

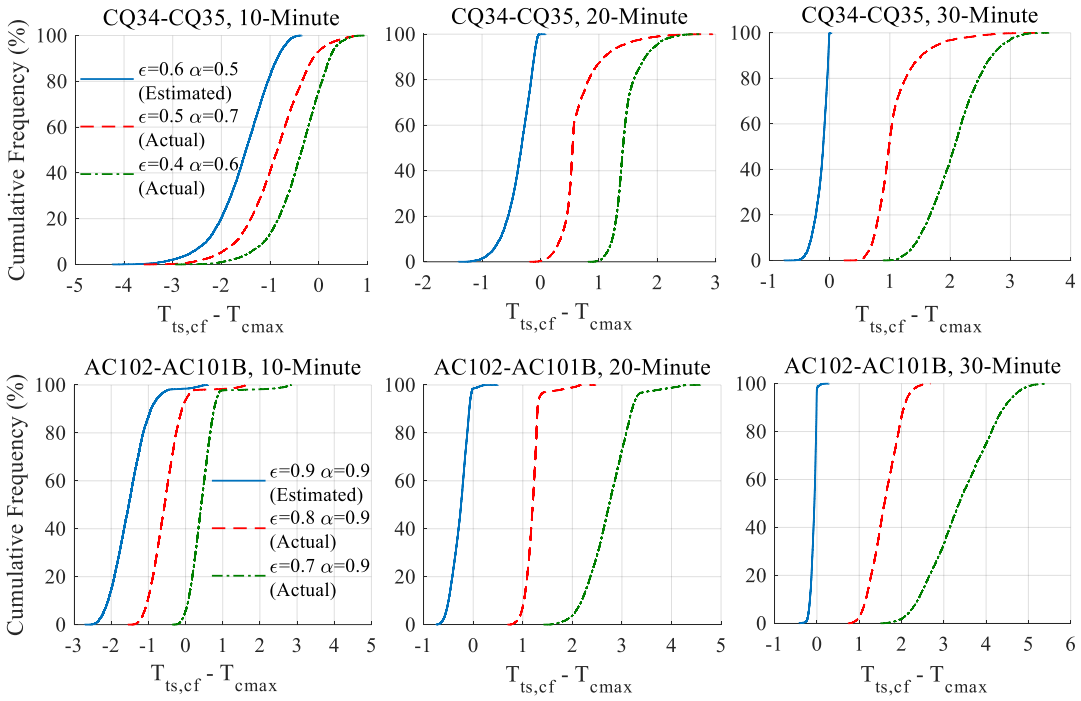

Fig. 11. Cumulative frequency distributions of deviations between T_{cmax} and $T_{ts,cf}$ tracked by the $T_{cav,\Delta t}$-based conventional approach with a 10-second Δt under the enhanced analytical method based transient ratings for different time horizons considering the estimation errors in the conductors' emissivity ϵ or absorptivity α for the two spans.

The $T_{cav,\Delta t}$-based conventional approach with a 10-second Δt is adopted as the benchmark in this work and also used to produce the 'actual' T_c from measured weather conditions and line currents. In practical application, some form of conductor temperature monitoring technique (e.g. Power Donut [21] that measures T_c at the fixed point without the need of a line outage for installation) should be available to validate the calculated 'actual' T_c and calibrate the conductor characteristic parameters (e.g. ϵ and α) used in the thermal model of the conductor. For example, the value of ϵ was determined to minimize the average difference between the measured and simulated T_c for night-time periods in [22]. CIGRE Technical Brochure 299 [20] recommended that the value of α could be set to be 0.1 higher than the estimated value of ϵ.

5. Conclusions and future work

This paper has proposed a weather-based approach to probabilistic transient-state real-time thermal rating (RTTR) forecasts for overhead lines (OHLs) based on an enhanced analytical method for transient-state conductor temperature estimation. To further reduce computation time, a fast root-finding algorithm, i.e. the secant method, is used to find the steady-state final

conductor temperature corresponding to the line current and weather conditions after step changes, and to adjust the short-term RTTR until the conductor temperature reaches the maximum limit at the end of the specified period. The developed methods have been tested on two spans comprising different types of conductors. Since the conductor temperature is overestimated by the enhanced analytical method for the majority of the time, the enhanced analytical method based transient-state RTTR is generally conservative. Although the point RTTR forecasts show a higher accuracy than those that are derived from persistence forecasts of weather conditions, they are generally overestimated at low rating levels. This problem can be overcome by the adoption of a certain low percentile from a probabilistic RTTR forecast. The transient-state RTTR percentiles for a particular span derived from the correlated random weather samples generated from the conditionally heteroscedastic forecasting models are preferred in this study due to their improved calibration at the lower percentiles for time horizons of 20 and 30 minutes. This is because the significant positive correlations among random weather samples of the same parameters at different future moments expand the predictive distributions of 20-minute and 30-minute RTTRs.

Building on the present work, the proposed methods should be extended to determine the percentiles of transient rating forecasts for the entire OHL, using spatial interpolation methods to infer random weather samples experienced at all spans. The positive correlations among the same weather parameters at different stations added into random samples might expand the predictive distributions of transient ratings of an OHL, as the positive correlations among the same parameters at different future moments do for a particular span. Further work will apply the developed method to longer forecast time horizons. However, given a longer time for a conductor to respond to the change in line current and an increase in the forecast error with an increased time horizon, a long time horizon forecast of transient rating is unlikely to give much enhancement over the steady-state RTTR. Furthermore, the analytical method enhanced in this paper could be refined further to increase the accuracy of transient conductor temperature estimation. In addition, building on work in [6], the practical application value of predictive percentiles of transient ratings will be investigated in future work.

Acknowledgement

Support for the work described in this paper is gratefully acknowledged from the Energy Technology Partnership, Scottish Power Energy Networks and National Grid Electricity Transmission.

Reference

[1] C.F. Price and R.R. Gibbon, "Statistical approach to thermal rating of overhead lines for power transmission and distribution," in *Proc. Inst. Electr. Eng. C, Gen. Transm. Distrib.*, vol. 130, no. 5, pp.245-256, 1983.

[2] *IEEE Standard for Calculating the Current-Temperature of Bare Overhead Conductors*, IEEE Standard 738, 2012.

[3] CIGRE Work. Group B2.43, "Guide for thermal rating calculations of overhead lines," CIGRE, Pairs, Tech. Brochure 601, Dec. 2014.

[4] CIGRE Work. Group B2.36, "Guide for application of direct real-time monitoring systems," CIGRE, Paris, Tech. Brochure 498, Jun. 2012.

[5] S. Uski-Joutsenvuo, R. Pasonen, and S. Rissanen, "Maximising power line transmission capability by employing dynamic line ratings – technical survey and applicability in Finland," VTT Technical Research Centre of Finland, Espoo, Finland, Tech. Rep. 2013.

[6] F. Fan, K. Bell, and D. Infield, "Probabilistic real-time thermal rating forecasting for overhead lines by conditionally heteroscedastic auto-regressive models," *IEEE Trans. Power Del.*, vol. 32, no. 4, pp. 1881-1890, Aug. 2017.

[7] X. Sun, P.B. Luh, K.W. Cheung, and W. Guan, "Probabilistic forecasting of dynamic line rating for over-head transmission lines," *2015 IEEE Power & Energy Society General Meeting*, pp. 1-5, 2015.

[8] N. Balu, T. Bertram, A. Bose, V. Brandwajn, G. Cauley, D. Curtice, A. Fouad, L. Fink, M.G. Lauby, B.F. Wollenberg, and J.N. Wrubel, "On-line power system security analysis," *Proceedings of the IEEE*, vol. 80, no. 2, pp. 262-282, 1992.

[9] M. Belivanis and K.R.W. Bell, "Coordination of the settings of phase-shifting transformers to minimize the cost of generation re-dispatch," *45th CIGRE Session*, Paris, paper C2-204, Aug. 2014.

[10] V.T. Morgan, *Thermal Behaviour of Electrical Conductors: Steady, Dynamic & Fault-Current Ratings*. Somerset, U.K.: Research Studies Press, 1991.

[11] A. Michiorri, P.C. Taylor, SC.E. Jupe, and C.J. Berry, "Investigation into the influence of environmental conditions on power system ratings," in *Proc. IMechE A: J. Power Energy*, vol. 223, pp. 743-757, Nov. 2009.

[12] *Implementation of Real-Time Thermal Ratings*, Scottish Power Energy Networks, Final Close Down Rep. LCNF SPT1001, Glasgow, 2013.

[13] J. Lambers, *Lect. Notes The Secant Method*, Univ. Southern Mississippi, Mississippi, USA, 2010. http://www.math.usm.edu/lambers/mat772/fall10/lecture4.pdf

[14] R.Y. Rubinstein and D.P. Kroese, *Simulation and the Monte Carlo Method*, 2nd, Hoboken, NJ, USA: Wiley, 2007.

[15] R.L. Iman and W.J. Conover, "A distribution-free approach to inducing rank correlation among input variables," *Commun. Stat.–Simul. Copmut.*, vol. 11, no. 3, pp. 311-334, 1982.

[16] B.E. Hansen, *Lect. Notes Nonparametrics*, Univ. Wisconsin, Madison, WI, USA, 2009.

https://pdfs.semanticscholar.org/2c36/60a1844f55935f7 98b10a48197a665d1a825.pdf

[17] *MATLAB Release 2017a*, The MathWorks, Inc. Natick, MA, USA.

[18] F. Fan, K. Bell, and D. Infield, "Probabilistic weather forecasting for dynamic line rating studies," *Power Syst. Comput. Conf.*, pp. 1-7, 2016.

[19] J. Hosek, P. Musilek, E. Lozowski, and P. Pytlak, "Effect of time resolution of meteorological inputs on dynamic thermal rating calculations," *IET Gen. Transm. Distrib.*, vol. 5, no.9, pp.941-947, 2011.

[20] CIGRE Work. Group B2.12, "Guide for selection of weather parameters for bar overhead conductor ratings," CIGRE, Tech. Brochure 299, 2006.

[21] *Power Donut 3: PD3 Instrumentation Platform for Overhead Transmission Lines*, Underground Systems Inc., Connecticut, USA, Jan. 2017.

[22] J. Rodriguez Alvarez, J. Azurza Anderson, and C.M. Franck, "Validation of a thermal model for overhead transmission lines at high conductor temperature," *IEEE PEC General Meeting*, Jul. 2016.

Appendix: Technical parameters of conductors

Conductor Characteristics	ACSR 'Drake'	ACSR 'Lynx'	AAAC 'Poplar'
Conductor diameter (mm)	28.143	19.53	20.09
Emissivity (-)	0.8	0.6	0.9
Solar absorptivity (-)	0.8	0.5	0.9
Low/high conductor temperature for which ac resistance is specified (℃)	25 / 75	20 / 45	20 / 70
Conductor ac resistance at low/high conductor temperature (Ω/km)	0.0727 / 0.0872	0.1583 / 0.1740	0.1404 / 0.1600
Specific heat capacity of steel/aluminium at 20℃ (J/(kg· ℃))	481 / 897		
Temperature coefficient of steel/aluminium specific heat capacity (1/℃)	$1.00\cdot 10^{-4}$ / $3.80\cdot 10^{-4}$		
Steel/aluminium mass per unit length (kg/m)	0.5119 / 1.116	0.335 / 0.507	- / 0.659
Conductor elevation above sea level (m)	0	16.7	36.6
Conductor orientation (degree counter-clockwise rotation from East)	N/A	35.4525	167.0054
Reduced maximum allowable conductor temperature (℃)	N/A	45	70
Static line rating for Winter/Spring or Autumn/Summer (A)	N/A	485 / 450 / 389	607 / 581 / 533